Journal of Materials in Civil Engineering. Submitted April 15, 2012; accepted December 5, 2012; posted ahead of print December 7, 2012. doi:10.1061/(ASCE)MT.1943-5533.0000754

Multiscale Chemo-Thermo-Hydro-Mechanical Modeling of Early Stage Hydration and Shrinkage of Cement Compounds

Zhen Liu[1] and Xiong Yu[2*]

Downloaded from ascelibrary.org by CASE WESTERN RESERVE UNIV on 01/10/13. Copyright ASCE. For personal use only; all rights reserved.

Abstract

The early stage cement hydration is critical to the strength and durability of cement-based materials. Due to the complex processes involved, holistic multiphysics and multiscale simulation is challenging. This paper introduces the concept of water characteristic curve (WCC) used in unsaturated soils to cement-based materials. The WCC characterizes the internal structure of cement and essentially relates the pore morphology and physical chemistry of solid-liquid interface in microscale to the concepts of suction and water content in macroscale. A thermo-hydro-mechanical model was developed based on this multiscale technique. A modified Fourier's heat equation for the thermal field, a modified Richards' equation for the hydraulic field, and an extended Navier's equation for the mechanical field were employed for developing the theoretical multiphysics framework. Auxiliary relationships, e.g., temperature-induced flow, chemical reaction information of cement components, were adopted for the completeness of the formulation. This simulation framework was implemented with the finite element method. Phenomena such as shrinkage, which is typical of early stage cement hydration process, were reproduced. The methodology of this model provides a solid corner stone for the simulation-based prediction of concrete performance.

Keywords: Multiphysics, Multiscale, Chemico-thermo-hydro-mechanical, Early stage cement hydration, Autogenous shrinkage

Accepted Manuscript Not Copyedited

Introduction

Concrete is one of the most widely used man-made materials in the world (Gartner 2004). It is an essential component of our infrastructures due to its excellent performance. However, the serviceability and durability of concrete are harmed by the defects and cracks resulting from the early stage concrete shrinkage (Holt and Leivo 2004; Bazant and Raftshol 1982). The volume changes, mostly chemical shrinkage, commence right after the concrete mixing and develop with cement hydration. They are unavoidable even if ideal curing conditions are provided. The countermeasure is to take proper engineering actions (i.e., saw cutting) prior to

[1] Graduate Assistant, Department of Civil Engineering, Case Western Reserve University, 2104 Adelbert Road, Bingham 256, Cleveland, OH 44106-7201, zhen.liu@case.edu.

[2]*Associate Professor, Department of Civil Engineering, Case Western Reserve University, 2104 Adelbert Road, Bingham 206, Cleveland, OH 44106-7201, xxy21@case.edu

Copyright 2012 by the American Society of Civil Engineers

Journal of Materials in Civil Engineering. Submitted April 15, 2012; accepted December 5, 2012; posted ahead of print December 7, 2012. doi:10.1061/(ASCE)MT.1943-5533.0000754

Downloaded from ascelibrary.org by CASE WESTERN RESERVE UNIV on 01/10/13. Copyright ASCE. For personal use only; all rights reserved.

the initiation of shrinkage cracks.

Concrete shrinkages can be categorized as drying shrinkage, autogenous shrinkage, thermal expansion and carbonation shrinkage according to their mechanisms (Holt and Leivo 2004). All these four types of shrinkages happen both in the early age (<24 hours) and in the late age (>24 hours) (Holt and Leivo 2004). Concrete at these two stages experiences distinctive changes in its microstructure. Consequently, the relative contributions of a specific type of shrinkage can be different at different curing stages.

In general, shrinkage in the early stage is more intricate due to the dramatic structural change. Upon pouring, concrete evolves from a mixed liquid state to a setting state with a developing skeleton and then gradually to a hardening semi-solid. At the very beginning, autogenous shrinkage is the same as chemical shrinkage as the fresh cement has no strength to resist deformations. But once a skeleton starts to develop from hydration products (Calcium Silicate Hydrates, or CSH) between 4 and 8 hours after mixing, autogenous shrinkage as an external shrinkage is no more the same as chemical shrinkage. This is because water is no longer free to be drawn out of voids in the skeleton. Menisci occur in these voids when a part of water is sucked to neighboring reaction sites. In the meanwhile, the pressure differences across these menisci exert tension on the skeleton in terms of suction. The consequent autogenous shrinkage is turning out to be a smaller and smaller portion of the chemical shrinkage. This process is similar to the drying process of other porous materials such as soils. That is, the system potential changes with water content, which is responsible for other changes such as water migrations, energy transfers and volume changes.

Most of the aforementioned aspects of concrete shrinkage can be simulated once a multiphysics model with properly formulated boundary conditions is available. But different shrinkage components are associated with different coupling effects. For the drying shrinkage, significant factors of interest include the water bleedings resulting from the density difference of aggregates and water, and the water migration affected by the varying hydraulic conductivity and the evaporation. And the rate of evaporation is determined mostly by external curing conditions such as the wind speed, temperature, and humidity. For autogenous shrinkage, the main concern is a quantitative description of the self-desiccation process. Shrinkage develops as a result of the increasing suction from decreasing water. While for thermal shrinkage, the focus is the temperature rise due to the enthalpy released by hydration reactions. In all of the above concerns, the evolution of mechanical properties needs to be considered. In summary, to model the hydration effects on early stage concrete behaviors, the decreasing water content must be considered in the relevant thermal, hydraulic, chemical and mechanical fields. Therefore, a coupled thermo-hydro-mechanical model including chemical kinetics is the key to predict the cement hydration process and its engineering effects on early stage concrete behaviors.

Attempts have been made to explore the use of multiphysics, especially the couplings effects in the chemico-thermo-mechanical field, in the early stage hydrations of cement-based materials (Schrefler et al. 2002; Lackner et al. 2002). These studies were conducted based on the mixture theory rather than the intrinsic characteristic of cement-based materials, which are porous materials consisting of solid matrix, internal pore structures, and fluid phases. The

Copyright 2012 by the American Society of Civil Engineers

Accepted Manuscript Not Copyedited

Journal of Materials in Civil Engineering. Submitted April 15, 2012; accepted December 5, 2012; posted ahead of print December 7, 2012. doi:10.1061/(ASCE)MT.1943-5533.0000754

Downloaded from ascelibrary.org by CASE WESTERN RESERVE UNIV on 01/10/13. Copyright ASCE. For personal use only; all rights reserved.

multiscale features which connect the characteristics in microscale such as pore space morphology and surface chemistry to the suction and deformation concepts in continuum mechanics are thus unable to be captured. A multiscale and multiphysics model based on the intrinsic characteristic is necessary to further advance the understanding of the behaviors of the early stage cement-based materials. Such a holistic model will allow the coupling effects, e.g. suction induced autogenous shrinkage, which have be repeatedly confirmed and simulated with phenomenological methods (Hua et al. 1995; Lura et al. 2003), to be realistically reproduced. Therefore, this innovative methodology will be an important simulation based engineering tool.

In this paper, we extended the concept of water characteristic curve, which has been mainly applied in unsaturated soils, to the early stage cement. The WCC represents a multiscale concept that links pressures measured in the macroscale to the microscale pore structure and the physical chemistry information. A theoretical framework for the early stage cement hydration is presented, which includes the coupling of the thermal field, hydraulic field, mechanical field as well as chemical kinetics imported from experimental data. The theoretical model is implemented with the Finite Element Method (FEM). Computational results show that the model can realistically reproduce observed shrinkage behaviors in the hydrating cement.

Characterization of Cement Paste with Water Characteristic Curve

It is well known that cement-based materials can be viewed as a porous material with multiscale structures from nano-scale to macro-scale (Ulm et al. 2004). This truth is partly attributable to the fact that cement itself consists of pores from intra-globules nanoporosity of several nanometers to entrained air voids of several millimeters (Ulm et al. 2004; Mehta and Monteiro 1993). Menisci arise when some of these internal pores are partially saturated with liquids such as water. A pressure difference across the vapor-liquid interface then appears due to the presence of the menisci. Subsequently, suction is developed and results in volume changes. On the other hand, water imbibitions are easier to occur in pores of smaller size which corresponds to higher suction. Therefore, if the variation of pore spaces is insignificant during imbibitions, there is a unique relationship between the water content (or saturation) and matric suction (air pressure minus water pressure), which can be called WCC. The existence and uniqueness of this relationship have been confirmed in general porous materials as a ternary system (solid, liquid, and gas). The WCC is the derivative of the Helmholtz energy of the whole system with respect to the volume change of the pore fluid (Morrow 1970).

The WCC can be conveniently linked to the morphology of internal structure and surface physical chemistry by the Young-Laplace equation and the 'Bundle of Cylindrical Capillary' model (BCC model) (Mualem 1976). The purpose of this conceptual model (BCC) was achieved firstly by describing the pressure equilibrium within a water sorption process in a pore. The first step is to formulate the thermodynamics across the gas-liquid interface in this pore. Pressures of liquid and gas within porous material are connected to pore morphology by

Copyright 2012 by the American Society of Civil Engineers

Accepted Manuscript Not Copyedited

Journal of Materials in Civil Engineering. Submitted April 15, 2012; accepted December 5, 2012; posted ahead of print December 7, 2012. doi:10.1061/(ASCE)MT.1943-5533.0000754

Downloaded from ascelibrary.org by CASE WESTERN RESERVE UNIV on 01/10/13. Copyright ASCE. For personal use only; all rights reserved.

the Young-Laplace equation:

$$\Delta p = \gamma \nabla \cdot \mathbf{n} = \gamma \left(\frac{1}{r_1} + \frac{1}{r_2} \right) \tag{1}$$

where Δp is the pressure difference across the fluid interface, γ is the surface tension of the liquid, $\mathbf{n}$ is the unit outward normal vector of the fluid surface, and r_1, r_2 are principal radii of a two-dimensional surface.

In the BCC model, a porous medium is conceptualized as a bundle of cylindrical capillaries. Applying the equation to cylindrical capillaries, we obtain

$$p_\alpha - p_\beta = \frac{2\gamma \cos \theta_c}{r} \tag{2}$$

where p_α and p_β are the internal and external pressures of the spherical surface, r is its radius and θ_c is the liquid-solid contact angle. In order to make use of Eq. 2 in porous media, matric suction ψ is introduced as

$$\psi = p_L - p_V \tag{3}$$

where p_L, p_V are usually water (liquid) and air (gas) pressures in porous materials.

When the osmotic pressure caused by chemical potential of solvents in saline conditions is neglected, the matric suction equals the total suction. We thus can calculate total suction, or suction in short, in a cylindrical capillary during in a wetting/drying process as

$$\psi = \frac{2\gamma \cos \theta_c}{r} \tag{4}$$

Then the two particular suction conditions can be derived based on the above introduction (Fredlund and Xing 1994):

$$\psi_{max} = \frac{A}{r_{min}} \tag{5}$$

$$\psi_{aev} = \frac{A}{r_{max}} \tag{6}$$

where A is a constant which equals $2\gamma \cos \theta_c$. Therefore the maximum matric suction, ψ_{max}, corresponds to the minimum pore radius r_{min}; and the air-entry suction, ψ_{aev}, corresponds to the maximum pore radius R_{max}.

The saturation can be integrated from the pore volumes by Eq. 7 (Mualem 1976),

Accepted Manuscript Not Copyedited

Copyright 2012 by the American Society of Civil Engineers

Journal of Materials in Civil Engineering. Submitted April 15, 2012; accepted December 5, 2012; posted ahead of print December 7, 2012. doi:10.1061/(ASCE)MT.1943-5533.0000754

$$S(r) = \int_{r_{min}}^{r} f(x)V(x)dx \tag{7}$$

where S is the saturation, $f(r)$ is the probability density of the pore of radius r, $V(r)$ is the relative volume occupied by a single pore of radius r, and x is a dummy variable. Hence the saturated volumetric water content is reached with the maximum pore radius as Eq. 8.

$$S(r_{max}) = 1 \tag{8}$$

By combination of the above equations, the WCC can be obtained based on a pore-size distribution and physical chemistry of interfaces by Eq. 9 (Fredlund and Xing 1994).

$$S(\psi) = \int_{\psi_{min}}^{\psi} f(\frac{A}{y})V(y)d(\frac{A}{y}) = \int_{\psi}^{\psi_{max}} f(\frac{A}{y})V(y)\frac{A}{y^2}d(y) \tag{9}$$

where y is a dummy variable representing suction in the integration.

In cement, a porous solid skeleton forms after the percolation threshold (setting point). This skeleton keeps changing with the development of cement hydration. Newly formed hydration products such as CSH are produced in the pore spaces. Shown in Fig. 1a are the typical pore size distributions in cement pastes obtained by mercury intrusion porometry (Young 1974). As can be seen, there exists a pore size distribution at any specific time within a cement hydration process. And most of the pore volume is occupied by capillary pores from 0.01 micron to 10 microns. WCCs were developed with the above pore size distributions by means of the above theory (Eqs. 1-9) (in Fig. 1b). Four WCCs were obtained for the different pore size distributions at different times. It is encouraging to find out that all of the WCCs except that for the first day can be well fitted by van Genuchten's equation, which is conventionally used for describing the WCC (van Genuchten 1980). This verifies the validity of these WCCs for cement. The discrepancy in the curve fitting of the water characteristic curve for the first day may stem from the inaccuracy in the measurement of the pore-size distribution. This is because the errors in applying the mercury intrusion porosity can be greater as the solid skeleton is very unstable in the early stage (1 day). By now, a new concept for the characterization of cement was developed. The WCC also serves as a multiscale technique to link the Young's equation in microscale to macroscopic suction commonly used in continuum mechanics in macroscale. This technique enables the development of the chemico-thermo-hydro-mechanical formulation for cement hydration.

Transport Properties of Hydrating Cement

Once the WCC was determined, other parameters, e.g., the hydraulic conductivity can be obtained. And these parameters are necessary for a thermo-hydro-mechanical formulation. The hydraulic conductivity was obtained by means of a relative permeability function which

Copyright 2012 by the American Society of Civil Engineers

Downloaded from ascelibrary.org by CASE WESTERN RESERVE UNIV on 01/10/13. Copyright ASCE. For personal use only; all rights reserved.

Accepted Manuscript Not Copyedited

Journal of Materials in Civil Engineering. Submitted April 15, 2012; accepted December 5, 2012; posted ahead of print December 7, 2012. doi:10.1061/(ASCE)MT.1943-5533.0000754

Downloaded from ascelibrary.org by CASE WESTERN RESERVE UNIV on 01/10/13. Copyright ASCE. For personal use only; all rights reserved.

was integrated from a WCC using Eq. 10 (Fredlund et al. 1994) as

$$K = K_0 \cdot \frac{\int_{\ln(h)}^{b} \frac{\theta_w(e') - \theta_w(h)}{e'} \theta_w'(e')\,dy}{\int_{\ln(h_{aev})}^{b} \frac{\theta_w(e') - \theta_s}{e'} \theta_w'(e')\,dy} \tag{10}$$

where K is the hydraulic conductivity, K_0 is the saturated hydraulic conductivity, b equals $\ln(1000000)$ (Fredlund et al. 1994), y is a dummy variable of integration representing the logarithm of suction, h_{aev} is the air entry value of suction in kPa, θ_w is the volumetric water content, θ_s is the volumetric saturated water content. θ_w is readily available once the saturation and porosity are known.

The thermally-induced water flow results from the temperature dependence of the non-isothermal WCC. It is usually taken into account as an additional hydraulic conductivity, K_T, by Eq. 11 (Hansson et al. 2004). This equation was developed from the thermodynamics theory proposed by Philip and de Vries (1957).

$$K_T = K \cdot \left(G \frac{\psi}{\gamma_0} \frac{d\gamma}{dT} \right) \tag{11}$$

where T is temperature, γ denotes the surface tension of soil water, which varies with temperature and can be approximated by $\gamma = 75.6 - 0.1425T - 2.38\times10^{-4}T^2$; γ_0 is the value of γ at 25 °C, iz. $\gamma_0 = 71.89\times10^{-3}\ \mathrm{N\cdot m^{-2}}$. G_{wt} is proposed frequently as a gain factor since some researchers maintained that surface tension as the unique factor considered by temperature by Philip and de Vries (1957) underestimates this temperature effect. Values such as 7 can be assigned for coarse-grained soils (Noborio et al. 1996). Here we assumed the contact angle to be zero because of the high surface energy of the cement components. The gain factor is thus assumed to be 1 in the process of cement paste hydration.

Theoretical Formulation of the Multiphysics

Thermal Field

The thermal migration was comprehensively described by the Fourier's equation with both conduction and convection terms (Eq. 12). The enthalpy changes caused by the hydration reactions were incorporated as a heat source term.

Copyright 2012 by the American Society of Civil Engineers

Accepted Manuscript Not Copyedited

Journal of Materials in Civil Engineering. Submitted April 15, 2012; accepted December 5, 2012; posted ahead of print December 7, 2012. doi:10.1061/(ASCE)MT.1943-5533.0000754

$$C\frac{\partial T}{\partial t}+\nabla\cdot\left(-\lambda\nabla T\right)=-C_w\nabla\left(\mathbf{J}T\right)+S_{heat} \tag{12}$$

where C is the overall volumetric heat capacity and λ is the overall thermal conductivity of cement paste, T is temperature, t is time, C_w is the volumetric heat capacity of water and $\mathbf{J}$ is the water flux from the hydraulic field. Both C and λ are coupling variables. The moisture migration changes the cement composition and consequently changes C and λ, which in return affect the heat transfer process. S_{heat} is the energy source (rate) resulting from the chemical reactions and can be formulated by Eq. 13.

$$S_{heat}=\sum S_{heat,J}=\sum-\frac{d\left(\theta_J h_J\right)}{dt} \tag{13}$$

where θ_J and h_J are the volume fraction and volumetric specific enthalpy change of the hydration reaction of phase *J*, respectively. *J* is a dummy index, which denotes cement components, i.e., C_3S, C_2S, C_3A or C_4AF, throughout the paper. The average heat capacity was calculated as a volume average value as Eq. 14,

$$C=C_w\theta_w+\sum C_J\theta_J \tag{14}$$

where C_J is the volumetric heat capacity of phase *J*. The thermal conductivity can be approximated by employing a homogenization approach as Eq. 15 (de Vries 1963),

$$\lambda=\frac{\lambda_w\theta_w+\sum\lambda_J\theta_J\left[1+\left(\lambda_w/\lambda_J\right)/3\right]^{-1}}{\theta_w+\sum\theta_J\left[1+\left(\lambda_w/\lambda_J\right)/3\right]^{-1}} \tag{15}$$

where λ_w is the thermal conductivity of water, and λ_J is the conductivity of phase *J*. But it has also been reported that the thermal conductivity of cement paste does not change significantly in at early stage. Thus a constant value such as unity can be alternatively adopted (Bentz 2008).

Hydraulic Field

For variably unsaturated porous media, the fluid movement is generally described by the mix-type Richards' equation, which has been shown to have a good performance in mass conservation (Celia and Binning 1992). A modified Richards' equation as Eq. 16 is adopted.

Copyright 2012 by the American Society of Civil Engineers

Downloaded from ascelibrary.org by CASE WESTERN RESERVE UNIV on 01/10/13. Copyright ASCE. For personal use only; all rights reserved.

Accepted Manuscript Not Copyedited

Journal of Materials in Civil Engineering. Submitted April 15, 2012; accepted December 5, 2012; posted ahead of print December 7, 2012. doi:10.1061/(ASCE)MT.1943-5533.0000754

$$\frac{\partial \theta_w}{\partial t} + \nabla \cdot \left(K_{Lh} \nabla \psi + K_{Lh} \mathbf{i} + K_{LT} \nabla T \right) = -S_{mass} \tag{16}$$

where K_{Lh} is the hydraulic conductivity, K_{LT} is the hydraulic conductivity due to thermal gradients, $\mathbf{i}$ is the unit vector along the direction of gravity, S_{mass} is the water consumption rate due to self-desiccation (mass sink) which is calculated using Eq. 17,

$$S_{mass} = \sum \left(\frac{d\theta_J}{dt} \cdot R_J \right) \tag{17}$$

where R_J is the volume ratio of water to the phase *J* in individual hydration reactions.

Mechanical Field

The continuum formation of the mechanical behaviors consists of the construction of the equation of motion, the strain-displacement correlation, and the constitutive relationship. A comprehensive mechanical model was established to describe the mechanical responses of the early stage cement paste. The equation of equilibrium (Eq. 18) was introduced in general tensor format in the first step.

$$\nabla \cdot \boldsymbol{\sigma} + \mathbf{F} = 0 \tag{18}$$

Strain-displacement equation is:

$$\boldsymbol{\varepsilon} = \frac{1}{2} \left[\nabla \mathbf{u} + (\nabla \mathbf{u})^T \right] \tag{19}$$

Constitutive equation is:

$$\boldsymbol{\sigma} = \mathbf{D} : \boldsymbol{\varepsilon} \tag{20}$$

where $\boldsymbol{\sigma}$ is the Cauchy stress tensor, $\boldsymbol{\varepsilon}$ is the infinitesimal strain tensor, $\mathbf{u}$ is the displacement vector, $\mathbf{D}$ is the fourth-order tensor of material stiffness, $\mathbf{F}$ is the body force per unit volume, the colon represents the double-dot product.

In order to consider the influences of the thermal field and hydraulic field on the mechanical field, the constitutive relationship for porous materials has to be established as Eq. 21,

$$\boldsymbol{\varepsilon} = \boldsymbol{\varepsilon}_{el} + \boldsymbol{\varepsilon}_{th} + \boldsymbol{\varepsilon}_{\psi} + \boldsymbol{\varepsilon}_0 \tag{21}$$

where $\boldsymbol{\varepsilon}_{el}$ is the elastic strain, $\boldsymbol{\varepsilon}_{th}$ is the strain caused by thermal expansion (Eq. 22), $\boldsymbol{\varepsilon}_{\psi}$ is the strain resulting from the change of the matrix suction, $[\psi / H, \psi / H, 0]^T$, H is a the modulus corresponding to matric suction, $\boldsymbol{\varepsilon}_0$ is the initial strain.

Copyright 2012 by the American Society of Civil Engineers

Downloaded from ascelibrary.org by CASE WESTERN RESERVE UNIV on 01/10/13. Copyright ASCE. For personal use only; all rights reserved.

Accepted Manuscript Not Copyedited

Journal of Materials in Civil Engineering. Submitted April 15, 2012; accepted December 5, 2012; posted ahead of print December 7, 2012. doi:10.1061/(ASCE)MT.1943-5533.0000754

$$\boldsymbol{\varepsilon}_{th} = \alpha\left(T - T_{ref}\right)\mathbf{I} \tag{22}$$

where $\mathbf{I}$ is $[1,1,1]^T$ for 2D models or $[1,1,1,1,1,1]^T$ for 3D models.

The coefficient of linear thermal expansion was approximated by a fitted relationship (Eq. 23) based on reported experimental data (Byfors 1980),

$$\alpha = 4.20835\times10^{-5}e^{-t/9.64962} + 0.052085e^{-t/0.05285} + 1.06784\times10^{-5} \tag{23}$$

where t is time in hour and α is in m/m. Two drained bulk moduli K and H were proposed for elastic stress and suction, respectively. The two moduli used here cast light on the role of pore pressure that was well considered in Biot's model for unsaturated soils with air bubbles and in Fredlund's method for addressing the volume change of unsaturated soils (Biot 1941; Fredlund and Rahardjo 1993). The value of H can be obtained via experiments.

Implementation

The theoretical framework outlined in the previous section includes three governing equations together with a collection of auxiliary equations. This equation system was solved with a finite element platform, COMSOL. However, in addition to the general information provided in the theoretical formulation section, more specific information is required. These pieces of information include chemical kinetics, constants for material properties, boundary and initial conditions, and other relationships and will be provided in this section.

Although chemical reactions in hydrated ordinary cement can be very complex according to Powers' work (Powers and Brownyard 1947), the reactions considered in this paper were restricted to the four basic ones defined by Eqs. (24-27) (Paulini 1992):

$$2C_3S + 6H \rightarrow C_3S_2H_3 + 3CH \tag{24}$$

$$2C_2S + 4H \rightarrow C_3S_2H_3 + CH \tag{25}$$

$$C_3A + 6H \rightarrow C_3AH_6 \tag{26}$$

$$C_4AF + 2CH + 10H \rightarrow C_3AH_6 + C_3FH_6 \tag{27}$$

The corresponding kinetics of the chemical reactions can be described by experimental curves as Fig. 2.

The basic input for the model is listed in the Table 1.

The volume fractions of cement components are functions of time and are dependent on their degrees of hydration. The volume fractions owe significant influences on the mass and heat source, and thus on the overall multiphysical process. The volume fractions were expressed by Eq. 28. In this simulation, the influence of volume strain was neglected by assuming that it does not contribute considerably to the total volume.

Copyright 2012 by the American Society of Civil Engineers

Downloaded from ascelibrary.org by CASE WESTERN RESERVE UNIV on 01/10/13. Copyright ASCE. For personal use only; all rights reserved.

Accepted Manuscript Not Copyedited

Journal of Materials in Civil Engineering. Submitted April 15, 2012; accepted December 5, 2012; posted ahead of print December 7, 2012. doi:10.1061/(ASCE)MT.1943-5533.0000754

$$\theta_J = \frac{m_J/\rho_J}{V_{total}} = \frac{\dfrac{(1-wc)\,\chi_J\,(1-\eta_J)}{\rho_J}}{(1+\varepsilon_v)\left[\dfrac{wc}{\rho_w}+\sum\dfrac{(1-wc)\,\chi_J}{\rho_J}\right]} \approx \frac{\dfrac{(1-wc)\,\chi_J\,(1-\eta_J)}{\rho_J}}{\left[\dfrac{wc}{\rho_w}+\sum\dfrac{(1-wc)\,\chi_J}{\rho_J}\right]} \tag{28}$$

where m_J, ρ_J, χ_J and η_J are the mass, density, initial mass fractions of clinkers and the degree of hydration of phase *J*, V_{total} is the total volume, ε_v is the volume strain, ρ_w is the water density and wc is mass fraction of water. wc was calculated from initial porosity and the mass fractions of clinkers by Eq. 29.

$$wc = \frac{\rho_w \theta_0 \sum \chi_J / \rho_J}{1-\theta_0+\rho_w\theta_0\sum \chi_J/\rho_J} \tag{29}$$

where θ_0 is the initial water content, which is 0.465 in this study. The average density of cement paste ρ was treated as a constant calculated with Eq. 30.

$$\rho = \frac{1}{\dfrac{wc}{\rho_w}+\sum\dfrac{(1-wc)\,\chi_J}{\rho_J}} \tag{30}$$

The chemical shrinkage was not incorporated in the multiphysics simulation but can be expressed by Eq. 31 for the purpose of the results evaluation (Paulini 1992). As an internal volume stain, the chemical shrinkage was negative as the total volume of solid and liquid decreases.

$$\begin{aligned}\varepsilon_{v,ca} = -[&53.2\cdot 3.14(1-\eta_{C_3S})\,\chi_{C_3S}/\rho_{C_3S} + 40\cdot 3.28(1-\eta_{C_2S})\,\chi_{C_2S}/\rho_{C_2S} \\ &+111.3\cdot 3.03(1-\eta_{C_3A})\,\chi_{C_3A}/\rho_{C_3A} + 178.5\cdot 3.8(1-\eta_{C_4AF})\,\chi_{C_4AF}/\rho_{C_4AF}]\end{aligned} \tag{31}$$

Autogenous shrinkage was calculated with the strain caused by suction. But if there is a moisture loss or gain through boundaries, Eq. 32 is more specifically designated for the shrinkage due to water loss. Both self-desiccation and moisture balance with environment are responsible for this water reduction under this condition.

$$\varepsilon_{v,w} = \int_{t=0}^{t} -\frac{d\psi(t)}{dt} H(t)\,dt \tag{32}$$

The above equation was derived by assuming that incremental model was applied during loading.

To avoid numerical difficulties such as singularities in stiffness matrices, a non-zero initial suction value, i.e., 5 kPa, was assumed. Consequently, parameters such as the elastic modulus were adjusted for calculations in the conditions of both small suction stress and

Copyright 2012 by the American Society of Civil Engineers

Downloaded from ascelibrary.org by CASE WESTERN RESERVE UNIV on 01/10/13. Copyright ASCE. For personal use only; all rights reserved.

Accepted Manuscript Not Copyedited

Journal of Materials in Civil Engineering. Submitted April 15, 2012; accepted December 5, 2012; posted ahead of print December 7, 2012. doi:10.1061/(ASCE)MT.1943-5533.0000754

Downloaded from ascelibrary.org by CASE WESTERN RESERVE UNIV on 01/10/13. Copyright ASCE. For personal use only; all rights reserved.

small elastic moduli in the fresh cement paste (Eq. 33). These treatments may result in some unexpected outcomes at the very beginning of numerical computations. But this influence faded out quickly with the rapidly increasing suction. Numerical stability was fairly guaranteed as suction got comparatively large.

$$H_{\text{hom}}=H_{\text{ult,hom}}\cdot\sum\eta_i\chi_i+\frac{3\psi}{\varepsilon_{v,cs}} \tag{33}$$

where H_{hom} is the homogenized drained bulk modulus with respect to suction while $H_{\text{ult,hom}}$ is the value of H_{hom} when cement is completely hydrated. *H* in Table 1 was calculated from the drained bulk modulus via a classical poroelastic relationship (Eqs. 34-35).

$$\sigma=K_{\text{hom}}\varepsilon+SB\psi \tag{34}$$

$$H_{\text{hom}}=\frac{K_{\text{hom}}}{SB} \tag{35}$$

where σ is the macroscopic mean stress, K_{hom} is the homogenized drained bulk modulus, ε is the volume strain, B is the Biot-Willis parameter.

The evaporation was formulated by a modified Penman equation (Shuttleworth 2007). The original equation was adopted with a minor modification as Eq. 39.

$$E_{\text{mm}}=F\frac{315.1952\frac{1}{T^2}\exp\left(21.07-\frac{5336}{T}\right)R_n+0.0278(1+0.536v_w)(1-h)\exp\left(21.07-\frac{5336}{T}\right)}{\frac{711.3955}{T^2}\left(21.07-\frac{5336}{T}\right)+0.0731} \tag{36}$$

where E_{mm} is in $\text{mm}\cdot\text{day}$, v_w is the wind speed in ms^{-1}, R_n is the net irradiance in $\text{MJm}^{-2}\text{day}^{-1}$, h is the relative humidity. A scaling factor F was employed because the original function was developed for pure water. In the following simulation, F was assumed to be unity to test the above function. Further calibrations are required to obtain the accurate expression of F.

The two dimensional computational domain was 27 cm wide and 10 cm high. It simulated a bulk of fresh cement paste poured into a smooth rigid box. Only the upper boundary was exposed to an environmental temperature of $20\,^{\circ}\text{C}$ and a water loss due to evaporation. All other boundaries were both thermal and hydraulic insulated. The simulation was initiated right after percolation. The initial temperature throughout the computational domain was 20 $^{\circ}\text{C}$.

Results and Analyses

Copyright 2012 by the American Society of Civil Engineers

Accepted Manuscript Not Copyedited

Journal of Materials in Civil Engineering. Submitted April 15, 2012; accepted December 5, 2012; posted ahead of print December 7, 2012. doi:10.1061/(ASCE)MT.1943-5533.0000754

Downloaded from ascelibrary.org by CASE WESTERN RESERVE UNIV on 01/10/13. Copyright ASCE. For personal use only; all rights reserved.

In this simulation, the fluid transfer through upper boundary was realized and formulated with the modified Penman's equation (Shuttleworth 2007). The influence of this boundary condition was evaluated prior to analyzing the dependent variables and the shrinkage components. From Fig. 3 we see that fluid evaporates from the boundary is responsible for less than 0.03 in the decrease of the volumetric water content. That is to say, this boundary condition was equivalent to a fairly good curing condition in which there is only a limited amount of water loss through the boundary.

The hydration process can affect the evaporation due to the decrease in the saturation and the change of the temperature. For example, the deviation of the evaporation curve from the linear curve correlates to certain extent with the temperature variation. However, these effects are discernible but insignificant. This is also observed in experimental results (Holt and Schodet 2002). The Penman's equation can be further improved to account for the effects of hydration on the evaporation, for example, by calibration.

The variations of the heat capacity of the cement composites have been proven to be appreciable during the early stage hydration (Bentz 2008). Therefore, the heat capacity was evaluated before checking other parameters since it has a great influence on the thermal field. The change in magnitude (from 2.4 to 1.6) agrees well with measured results (Bentz 2008). The deduction was attributed to the change in the composition which consequently led to a change in the overall heat capacity. Another parameter, hydraulic conductivity, was bypassed in most of the existing investigations. The reason is twofold: 1) the whole hydraulic field was customarily overlooked by directly assuming its effects are negligible, though the significance of the independent variable in the hydraulic field, suction, has been more and more recognized; 2) the basis for hydraulic field, that is, a system of a solid matrix and viscous fluids, has not been confirmed and well understood. If cement as a porous medium has not been recognized and characterized (moisture characteristic), the corresponding hydraulic field simulation is impossible. As illustrated in Fig. 4, the hydraulic conductivity decreased evidently by one order of magnitude. This proved that there was a considerable change in the hydraulic conductivity due to the fluid migration. The change is capable of altering the intensity of fluid transfer.

Plotted in Fig. 5 are the variations of the volumetric water content and that of the suction with respect to time. The volumetric water content decreased from 0.465 to 0.235. That is, around 50 percent (0.23/0.465) of water has been consumed by the chemical reactions and the water loss to ambient. Moreover, the variation of volumetric water content is relatively smooth within the whole range. This smooth decrease of water content agrees with the monitored phenomena (Holt 2001). However, there is a distinct increase in suction during the first hour of the hydration. This sudden increase was partly due to the comparatively higher intensity in hydration reactions when reactants come into contact; on the other hand, it also can be explained by the nonlinear relationship in the WCC at the low water content range. By comparison, it was found that the value of suction was greater than that cited in literature

Copyright 2012 by the American Society of Civil Engineers

Accepted Manuscript Not Copyedited

Journal of Materials in Civil Engineering. Submitted April 15, 2012; accepted December 5, 2012; posted ahead of print December 7, 2012. doi:10.1061/(ASCE)MT.1943-5533.0000754

Downloaded from ascelibrary.org by CASE WESTERN RESERVE UNIV on 01/10/13. Copyright ASCE. For personal use only; all rights reserved.

(Holt and Leivo 2004; Kronlof et al. 1995; Slowik et al. 2009). This is because in the suction measurement of early stage cement, the readings will decrease to zero once a suction meter encounters air bubbles (Slowik et al. 2009). This makes sense since this possibility increases as both the number and volumes of internal pores increase during cement hydration.

In Fig. 6a, the volume strains resulting from different mechanisms are illustrated. We can see that the volume strain caused by the thermal expansion appears as a volume increase. Its magnitude is bigger during the first hours of hydration. At this time, the thermal expansion was big enough to be considered as the predominant one. But it decreased later. And finally it was not comparable to the contribution from suction which was continuously increasing during the whole hydration. The increase of the volume strain actually includes the contributions from both the autogenous shrinkage and that from drying shrinkage. The comparison between the shrinkage due to suction and chemical shrinkage was comparable to both simulated results (Hua et al. 1995; Lura et al. 2003) and observed data (Kronlof et al. 1995; Koenders and van Breugel 1997). Moreover, the magnitude is also comparable. This is encouraging since the shrinkage components are the quantities of primary interest.

Macroscopic settlements also arouse interests in practice. Hence its variation is plotted with respect to time in Fig. 6b. Contrary to our general knowledge, the settlement appeared as a negative value (expand vertically) at the beginning. This can be explained by employing the results from volume strain analysis (Fig. 6a) for which the thermal expansion was noticeable during this time region. The settlement increased in absolute volume (magnitude) by the large. This phenomenon has also been observed in horizontal shrinkage (Kronlof et al. 1995). It is noted that the settlement caused by the density difference between water and clinkers was not incorporated in the current model. Finally, it is concluded that no specific pattern has been identified yet the settlement is closely related to the chemical reactions.

Internal stresses are responsible for the cracks in the early stage cement paste. If the developed stress exceeds the developed strength, cracks will be initiated. Therefore, the prediction of internal stress is very important. With the multiphysics simulation model developed in this work, the internal stress at any points within the cement paste can be predicted. For evaluation, the averaged first and third principal stresses over the computational domain are plotted in Fig. 7. Both of them increased as hydration continues. The cement paste is exposed to a high risk of cracking when the development of strength is unable to keep pace with this increase in internal stresses. The fluctuations in the simulation results might come from the instability caused by the low initial modulus of the hydrating cement. The model simulation can be utilized to predict the crack initialization in hydrating cement-based materials once the developments of the strength and fracture roughness are

Accepted Manuscript Not Copyedited

Copyright 2012 by the American Society of Civil Engineers

Journal of Materials in Civil Engineering. Submitted April 15, 2012; accepted December 5, 2012; posted ahead of print December 7, 2012. doi:10.1061/(ASCE)MT.1943-5533.0000754

Downloaded from ascelibrary.org by CASE WESTERN RESERVE UNIV on 01/10/13. Copyright ASCE. For personal use only; all rights reserved.

available.

Conclusions

This paper reviewed the characteristics of cement-based materials in light of general porous materials theory. The water characteristic curve, which is popular for soils, was extended for cement-based materials. From this, a unique relationship between the matric suction and saturation was identified. This led to a multiscale technique for connecting the Young's equation in microscale to macroscopic continuum mechanics. Based on the multiscale technique, a new thermo-hydro-mechanical model was developed for the early age cement-base materials. This multiscale and multiphysics framework includes the thermal field, hydraulic field and mechanical field as well as experimental results of chemical kinetics. Various auxiliary correlations for the basic mechanisms were presented to give a close form to the theoretical model. The theoretical model was implemented numerically under typical boundary conditions. The results proved that the theoretical model could be solved smoothly with limited computational efforts.

The results evaluation showed that the model captures very well both the basic features and the various coupling effects of early stage cement hydration. Specially, the obtained trend of shrinkage was comparable with either simulated results or experimental results. The simulation predicted the stress and strain development while curing, which shed light on the mechanism of crack initialization in early age cement-based materials. This model will be further extended to include phenomena such as creep and percolation. The final goal is a holistic simulation for early stage cement hydration.

References

Bazant, Z. P., and Raftshol, W. J. (1982). "Effect of cracking in drying and shrinkage specimens." *Cem. Concr. Res.*, 12, 209-226.

Bentz, D. P. (2008). "A review of early-age properties of cement-based materials." *Cem. Concr. Res.*, 38, 196-204.

Biot, M. A. (1941). "General theory of three-dimensional consolidation. *J. Appl. Phys.*, 12, 155-164.

Byfors, J. (1980). "Plain concrete at early ages." *Report FO 3:80*, Swedish Cem. and Concr. Res. Inst., Stockholm, Sweden.

Celia, M. A., and Binning, P. (1992). "A mass conservative numerical solution for two-phase flow in porous media with application to unsaturated flow." *Water Resour. Res.*, 28, 2819-2828.

De Vries, D. A. (1963). "Thermal properties of soils." *Physics of plant environment*, W. R. Van Wijk, eds, Holland Publication Company, Amsterdam.

Fall, M., Adrien, D., Celestin, J. C., Pokharel, M., and Toure, M. (2009). "Saturated hydraulic conductivity of cemented paste backfill." *Min. Eng.*, 22, 1307-1317.

Fredlund, D. G., and Rahardjo, H. (1993). *Soil mechanics for unsaturated soils*, John Wiley & Sons, Inc., New York.

Copyright 2012 by the American Society of Civil Engineers

Accepted Manuscript Not Copyedited

Downloaded from ascelibrary.org by CASE WESTERN RESERVE UNIV on 01/10/13. Copyright ASCE. For personal use only; all rights reserved.

Fredlund, D. G., and Xing, A. (1994). "Equations for the soil-water characteristic curve." *Can.Geotech. J.*, 31, 521-532.

Fredlund, D. G., Xing, A., and Huang, S.. (1994). "Predicting the permeability function for unsaturated soils using the soil-water characteristic curve." *Can. Geotech. J.*, 31, 533-546.

Gartner, E. (2004). "Industrially interesting approaches to "Low-CO_2" Cements." *Cem. Concr. Res.*, 34, 1489-1498.

Hansson, K., Simunek, J., Mizoguchi, M., Lundin, L., and van Genuchten, M. Th. (2004). "Water flow and heat transport in frozen soil: numerical solution and freeze-thaw applications." *Vadose Zone J.*, 3, 693-704.

Hedlund, H. (1996). "Stresses in high performance concrete due to temperature and moisture variations at early ages." licentiate thesis, Lulea Univ. of Technol., Lulea, Sweden, 1996.

Hewlett, P. C. (1998). *Lea's Chemistry of Cement and Concrete*, 4th Ed., Elsevier, Arnold, Great Britain, 1998.

Holt, E. (2001). *Early age autogenous shrinkage of concrete*. doctoral dissertation, Univ. of Washington, Seattle.

Holt, E., and Leivo, M. (2004). "Cracking risks associated with early age shrinkage." *Cem. Concr. Compos.*, 26, 521-530.

Holt, E., and Schodet, O. (2002). "Self-compacting concrete." *Rep. No. R1SU00380*, Technical Research Center of Finland, FI-02044 VTT, Finland.

Hua, C., Acker, P., and Ehrlacher, A. (1995). "Analyses and models of the autogenous shrinkage of hardening cement paste I. modelling at macroscopic scale." *Cem. Concr. Res.*, 25, 1457-1468.

Koenders, E. A. B., and van Breugel, K. (1997). "Numerical modeling of autogenous shrinkage of hardening cement paste." *Cem. Concr. Res.*, 27, 1489-1499.

Kronlof, A., Leivo, M., and Sipari, P. (1995). "Experimental study on the basic phenomena of shrinkage and cracking of fresh mortar." *Cem. Concr. Res.*, 25, 1747-1754.

Lackner, R., Hellmich, Ch., and Mang, H. A. (2002). "Constitutive modeling of cementations materials in the framework of chemoplasticity." *Int. J. Numer. Meth. Eng.*, 83, 2357-2388.

Lura, P., Jensen, O. M., and van Breugel, K. (2003). "Autogenous shrinkage in high-performance cement paste: an evaluation of basic mechanisms." *Cem. Concr. Res.*, 33, 223-232.

Mehta, P. K., Monteiro, J. M. (1993). *Concrete: structure, properties and materials*, 2nd Ed., Prentice Hall, Inc. Englewood Cliffs, New Jersey.

Morrow, N. R. (1970). "Physics and thermodynamics of capillary action in porous media." *Ind. & Eng. Chem*., 62, 32-56.

Mualem, Y. (1976). "A new model for predicting the hydraulic conductivity of unsaturated porous media." *Water Res. Res.*, 12, 513-522.

Noborio, K., McInnes, K. J., and Heilman, J. L. (1996). "Two-dimensional model for water, heat and solute transport in furrow-irrigated soil: I. theory." *Soil Sci. Soc. Am. J.*, 60, 1001-1009.

Paulini, P. A. (1992). "Weighing method for cement hydration." *9th Int. Congr. on the*

Copyright 2012 by the American Society of Civil Engineers

Accepted Manuscript Not Copyedited

Chemistry of Cement, New Delhi, Vol. IV.

Penman, H. L. (1948). "Natural evaporation from open water, bare soil and grass. *Proc. Roy. Soc. Lond. Math. Phys. Sci.* , 193, 1948, 120-145.

Philip, J. R., and de Vries, D. A. (1957). "Moisture movement in porous materials under temperature gradients." *EOS Trans. Am. Geophys. Union*, 38, 1957, 222-232.

Powers, T. C., and Brownyard, T. L. (1947). "Studies of the physical properties of hardened Portland cement paste." *Bulletin. No. 2*, Research Laboratory of Portland Cement Association, Skokie, IL, U.S, reprinted from *J. Am. Concr. Inst. (Proc.)*, 43, 101-132, 249-336, 469-505, 549-602, 669-712, 845-880, 933-992.

Schrefler, B. A., Majorana, C. E., Khoury, G. A., and Gawin, D. (2002). "Thermo-hydro-mechanical modelling of high performance concrete at high temperatures." *Eng. Comput.,* 19, 787-797.

Shuttleworth, W. J. (2007). "Putting the 'vap' into evaporation." *Hydrol.Earth Syst. Sci.*, 11, 210-244.

Slowik, V., Hubner, T., Schmidt, M., and Villmann, B. (2009). "Simulation of capillary shrinkage cracking in cement-like materials." *Cem. Concr. Compos.*, 31, 461-469.

Ulm, F. J., Constantinides, G., and Heukamp, F. H. (2004). "Is concrete a porous materials?- a multiscale investigation of poroelastic properties." *Mater.Struct.*, 37, 43-58.

Van Genuchten, M. Th. (1980). "A closed-form equation for predicting the hydraulic conductivity of unsaturated soil." *Soil Sci. Soc. Am. J.*, 44, 892-898.

Young, J. F. (1974). "Capillary porosity in hydrated tricalcium silicate pastes." *Pow. Technol*., 9, 173 -179.

Accepted Manuscript Not Copyedited

Downloaded from ascelibrary.org by CASE WESTERN RESERVE UNIV on 01/10/13. Copyright ASCE. For personal use only; all rights reserved.

Copyright 2012 by the American Society of Civil Engineers

Journal of Materials in Civil Engineering. Submitted April 15, 2012; accepted December 5, 2012;
posted ahead of print December 7, 2012. doi:10.1061/(ASCE)MT.1943-5533.0000754

List of Tables

Table 1 Constant parameters used in the simulation

Downloaded from ascelibrary.org by CASE WESTERN RESERVE UNIV on 01/10/13. Copyright ASCE. For personal use only; all rights reserved.

Accepted Manuscript
Not Copyedited

Copyright 2012 by the American Society of Civil Engineers

Journal of Materials in Civil Engineering. Submitted April 15, 2012; accepted December 5, 2012; posted ahead of print December 7, 2012. doi:10.1061/(ASCE)MT.1943-5533.0000754

Downloaded from ascelibrary.org by CASE WESTERN RESERVE UNIV on 01/10/13. Copyright ASCE. For personal use only; all rights reserved.

Table 1 Constant parameters used in the simulation

Input	Value	Description
ρ_w	1000 (kg/m^3)	Density of water
ρ_{C3S}	3140 (kg/m^3)	Density of C_3S
ρ_{C2S}	3280 (kg/m^3)	Density of C_2S
ρ_{C3A}	3030 (kg/m^3)	Density of C_3A
ρ_{C4AF}	3800 (kg/m^3)	Density of C_4AF
h_{C3S}	517 (kJ/kg)	Enthalpy change of C_3S hydration
h_{C2S}	262 (kJ/kg)	Enthalpy change of C_2S hydration
h_{C3A}	908 (kJ/kg)	Enthalpy change of C_3A hydration
h_{C4AF}	418 (kJ/kg)	Enthalpy change of C_4AF hydration
R_{C3S}	18*6/1000/(456*2/3140)=0.3718	Volume ratio of H_2O to C_3S
R_{C2S}	18*4/1000/(344*2/3280)=0.3433	Volume ratio of H_2O to C_2S
R_{C3A}	18*6/1000/(242/3030)=1.3522	Volume ratio of H_2O to C_3A
R_{C4AF}	18*10/1000/(718/3800)=0.6597	Volume ratio of H_2O to C_4AF
χ_{C3S}	70%	Mass fraction of C_3S in clinkers
χ_{C2S}	12%	Mass fraction of C_2S in clinkers
χ_{C3A}	10%	Mass fraction of C_3A in clinkers
χ_{C4AF}	8%	Mass fraction of C_4AF in clinkers
K_0	1×10^{-5} (m/s) (Fall et al. 2009)	Initial hydraulic conductivity
$E_{ult,hom}$	14.1 (GPa) (Ulm et al. 2004))	Ultimate homogenized Young's modulus
ν_{hom}	0.25	Homogenized Poisson's ratio
$H_{ult,hom}$	14.1/0.69=20.4348 (GPa) (Ulm et al. 2004)	Ultimate homogenized Biot's coefficient
C_w	$4.18\times10^{6}(m^3/K)$	Heat capacity of water
C_s	$0.75\times10^{6}(m^3/K)$	Heat capacity of the clinkers
λ	$1(W/(m\cdot K))$ (Bentz 2008)	Thermal conductivity of hydrated cement

Accepted Manuscript
Not Copyedited

Copyright 2012 by the American Society of Civil Engineers

Journal of Materials in Civil Engineering. Submitted April 15, 2012; accepted December 5, 2012;
posted ahead of print December 7, 2012. doi:10.1061/(ASCE)MT.1943-5533.0000754

Downloaded from ascelibrary.org by CASE WESTERN RESERVE UNIV on 01/10/13. Copyright ASCE. For personal use only; all rights reserved.

List of Figures

Accepted Manuscript
Not Copyedited

Copyright 2012 by the American Society of Civil Engineers

Figure 1

Journal of Materials in Civil Engineering. Submitted April 15, 2012; accepted December 5, 2012;
posted ahead of print December 7, 2012. doi:10.1061/(ASCE)MT.1943-5533.0000754

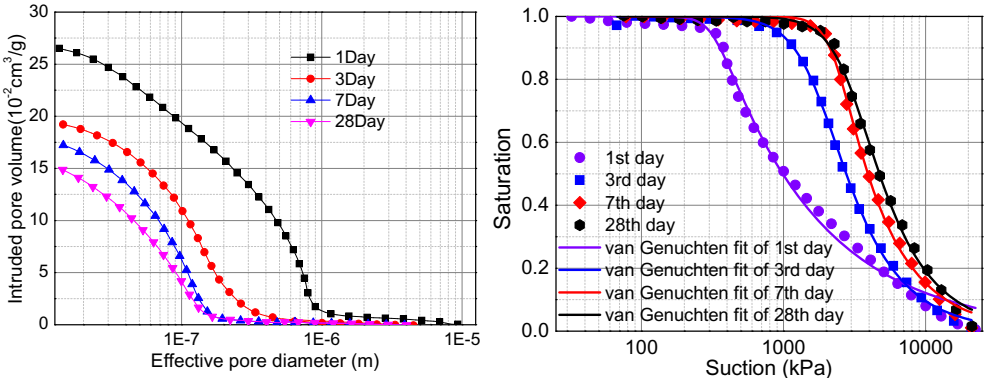

Fig. 1 a) Pore size distributions in cement paste at different curing ages (Young 1974); b) Estimated water characteristic curves at different curing ages using van Genuchten's equation (van Genuchten 1980)

Downloaded from ascelibrary.org by CASE WESTERN RESERVE UNIV on 01/10/13. Copyright ASCE. For personal use only; all rights reserved.

Accepted Manuscript
Not Copyedited

Copyright 2012 by the American Society of Civil Engineers

Figure 2

Journal of Materials in Civil Engineering. Submitted April 15, 2012; accepted December 5, 2012;
posted ahead of print December 7, 2012. doi:10.1061/(ASCE)MT.1943-5533.0000754

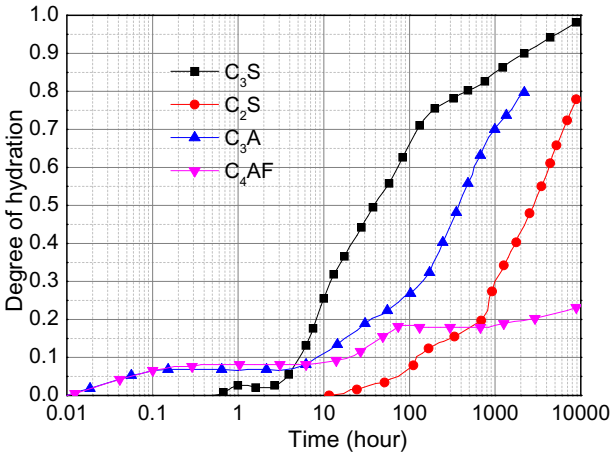

Fig. 2 Degree of hydration of cement compounds verse time from (Paulini 1992)

Downloaded from ascelibrary.org by CASE WESTERN RESERVE UNIV on 01/10/13. Copyright ASCE. For personal use only; all rights reserved.

Accepted Manuscript
Not Copyedited

Copyright 2012 by the American Society of Civil Engineers

Figure 3

Journal of Materials in Civil Engineering. Submitted April 15, 2012; accepted December 5, 2012;
posted ahead of print December 7, 2012. doi:10.1061/(ASCE)MT.1943-5533.0000754

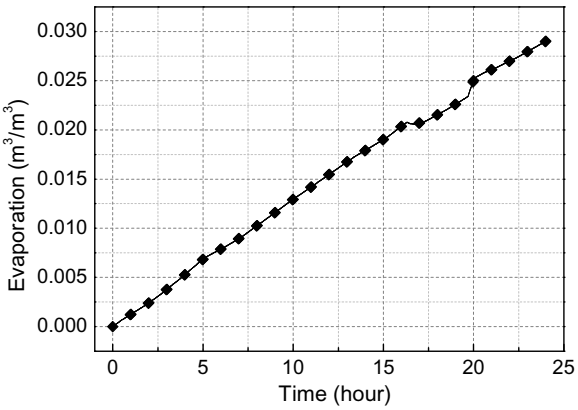

Fig. 3 Water decrease due to evaporation

Downloaded from ascelibrary.org by CASE WESTERN RESERVE UNIV on 01/10/13. Copyright ASCE. For personal use only; all rights reserved.

Accepted Manuscript
Not Copyedited

Copyright 2012 by the American Society of Civil Engineers

Figure 4

Journal of Materials in Civil Engineering. Submitted April 15, 2012; accepted December 5, 2012;
posted ahead of print December 7, 2012. doi:10.1061/(ASCE)MT.1943-5533.0000754

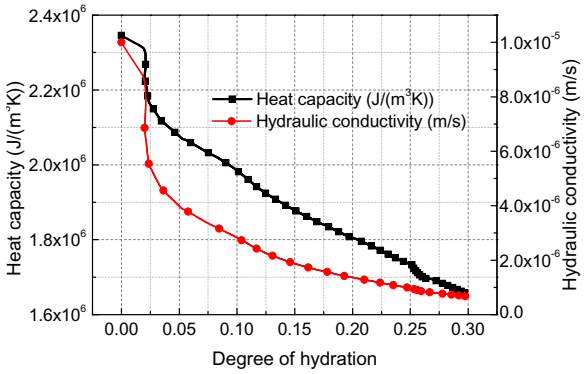

Fig. 4 Heat capacity and hydraulic conductivity of the cement composite at different degrees of hydration

Downloaded from ascelibrary.org by CASE WESTERN RESERVE UNIV on 01/10/13. Copyright ASCE. For personal use only; all rights reserved.

Accepted Manuscript
Not Copyedited

Copyright 2012 by the American Society of Civil Engineers

Journal of Materials in Civil Engineering. Submitted April 15, 2012; accepted December 5, 2012;
posted ahead of print December 7, 2012. doi:10.1061/(ASCE)MT.1943-5533.0000754

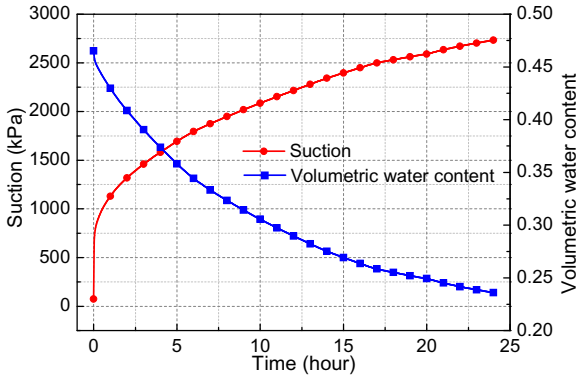

Fig. 5 Volumetric water content and suction versus time

Downloaded from ascelibrary.org by CASE WESTERN RESERVE UNIV on 01/10/13. Copyright ASCE. For personal use only; all rights reserved.

Accepted Manuscript
Not Copyedited

Copyright 2012 by the American Society of Civil Engineers

Journal of Materials in Civil Engineering. Submitted April 15, 2012; accepted December 5, 2012;
posted ahead of print December 7, 2012. doi:10.1061/(ASCE)MT.1943-5533.0000754

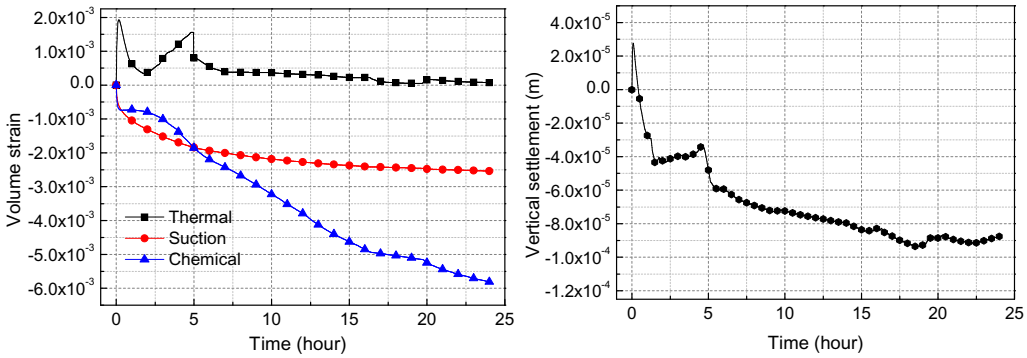

Fig. 6 a) Components of shrinkage in early stage cement hydration b) average vertical settlement

Downloaded from ascelibrary.org by CASE WESTERN RESERVE UNIV on 01/10/13. Copyright ASCE. For personal use only; all rights reserved.

Accepted Manuscript
Not Copyedited

Copyright 2012 by the American Society of Civil Engineers

Figure 7

Journal of Materials in Civil Engineering. Submitted April 15, 2012; accepted December 5, 2012;
posted ahead of print December 7, 2012. doi:10.1061/(ASCE)MT.1943-5533.0000754

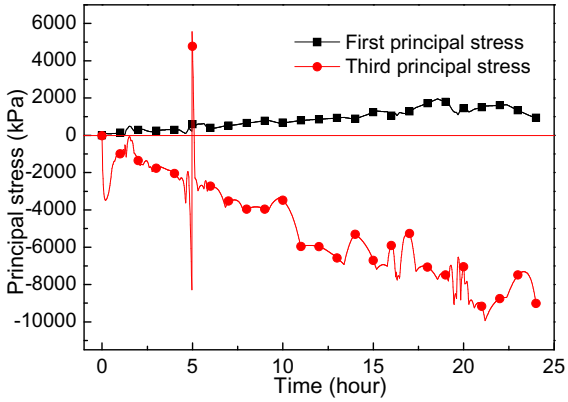

Fig. 7 Development of average internal stress

Downloaded from ascelibrary.org by CASE WESTERN RESERVE UNIV on 01/10/13. Copyright ASCE. For personal use only; all rights reserved.

Accepted Manuscript
Not Copyedited

Copyright 2012 by the American Society of Civil Engineers